Upconversion based spectral imaging in 6 to 8 m spectral regime

Junaid, Saher; Tidemand-Lichtenberg, Peter; Pedersen, Christian

Published in:
Proceedings of SPIE

Link to article, DOI:
10.1117/12.2250538

Publication date:
2017

Document Version
Publisher's PDF, also known as Version of record

Upconversion based spectral imaging in 6 to 8µm spectral regime

S. Junaid, P. Tidemand-Lichtenberg, C. Pedersen
Technical university of Denmark, Department of Fotonik Engineering, Frederiksborgvej 399, 4000 Roskilde, Denmark

ABSTRACT

Spectral imaging in the 6 to 8µm range has great potential for medical diagnostics. Here a novel technique based on frequency upconversion of the infrared images to the near visible for subsequent acquisition using a Si-CCD camera is investigated. The upconversion unit consists of an $AgGaS_2$ crystal and a 1064nm diode pumped solid state laser. A globar is used as mid-infrared illumination source. Acquired images contain both spectral and spatial information. Angle tuning of the nonlinear crystal is exploited to scan the phase match condition, which allows to cover the full spectral range of interest for the full field of view. Simulated images are created and compared with the measured images.

Keywords: Sum frequency generation (SFG), birefringence, non-collinear phase matching, spectral imaging.

INTRODUCTION

Mid infrared (MIR) detection has been center of attention for decades due to a multitude of applications in different fields such as environmental gas monitoring and biomedical studies [1] [2] [3] [4]. Fundamental absorption bands of many gases [5] and spectral features of many complex compounds is found in this spectral range. MIR spectral imaging has capability to distinguish between cancerous and healthy tissues and consequently the potential to be used for cancer diagnostics [6].

Lack of sensitive MIR detectors is a hurdle that has to be eliminated to take full advantage of this important spectral regime. The detectors being used presently for MIR detection are based on either microbolometer or InSb semiconductor technology which typically needs cryogenic cooling to minimize dark noise [7].

Nonlinear frequency upconversion of infrared images was demonstrated already in 1960 [8] but with very low conversion efficiency. The efficiency was improved drastically in 2012 where room-temperature mid-infrared single-photon spectral imaging was demonstrated using incoherent illumination sources in the 3µm spectral region [9]. Converting MIR to visible spectral range via nonlinear frequency upconversion allows for the use of silicon based detectors, thus enabling fast, sensitive and cheaper detection compared to MIR detection systems presently used.

Upconversion based MIR imaging has mainly been restricted below 5µm when using lithium niobate as the nonlinear material. Based on continuous wave (CW) upconversion and broadband MIR illumination, imaging and post processing for hyperspectral imaging has been demonstrated [10]. Also, upconversion based MIR imaging using pulsed illuminations sources has been shown [11] [12]. For the longer wavelength regime, upconversion technology has mainly been exploited for spectroscopic applications [13], however few papers have considered imaging at long IR wavelengths [14].

In this work, we demonstrate nonlinear frequency upconversion in the 6 to 8µm range for spectral imaging. The upconversion unit is a single-pass system consisting of an $AgGaS_2$ (AGS) crystal and a CW 1064nm laser as the mixing source.

Nonlinear Frequency Generation and Conversion: Materials and Devices XVI, edited by
Konstantin L. Vodopyanov, Kenneth L. Schepler, Proc. of SPIE Vol. 10088, 100880I

Incorporating scanning of the phase match condition allows us to cover full spectral range for the full field of view. Acquisition of spectral information from every pixel within the full field of view is important for specific application, such as medical diagnostics. There are different ways of scanning the phase match condition e.g. by temperature tuning, wavelength tuning of the mixing laser or by rotation of the nonlinear crystal. In the following, angle tuning of the nonlinear crystal is used to scan the phase match condition. Each image acquired at a specific phase match condition contains both spectral and spatial information. By taking a sequence of images while scanning the crystal rotation, a series of monochromatic images can be achieved after post processing.

The paper is structured in the following way; first the non-collinear frequency conversion theory is reviewed, then the setup is described. Finally, simulated and experimental results are presented, compared and discussed in detail.

THEORETICAL AND EXPERIMENTAL SETUP

The goal of the experiment is to exploit Sum Frequency Generation (SFG) to convert (MIR) radiations into visible part of the spectrum where Si based CCD cameras can be readily used for imaging. A setup demonstrating single-pass nonlinear frequency upconversion, exploiting birefringent non-collinear phase matching for spectral imaging, is presented using a globar as an illumination source.

The upconversion takes place in the Fourier plane of the object, meaning that the spatial information is encoded in angles; hence, non-collinear imaging needs to be considered. The phase match condition can be divided into longitudinal and transverse phase matching equations, where Δk_L represents the longitudinal phase mismatch and Δk_T the transverse phase mismatch.

$$\cos(\varphi_3)\frac{n_{e3}(\theta_3,\lambda_3)}{\lambda_3} - \frac{n_{o1}}{\lambda_1} - \cos(\varphi_2)\frac{n_{e2}(\theta_2,\lambda_2)}{\lambda_2} = \Delta k_L \tag{1}$$

$$\sin(\varphi_3)\frac{n_{e3}(\theta_3,\lambda_3)}{\lambda_3} - \sin(\varphi_2)\frac{n_{e2}(\theta_2,\lambda_2)}{\lambda_2} = \Delta k_T \tag{2}$$

Here λ_1, λ_2 and λ_3 is the mixing laser wavelength (1064nm), the MIR signal and upconverted wavelength respectively, θ_i is the angle between corresponding wave vectors k_i and optical axis of the crystal. φ_3 and φ_2 denotes the angles which upconverted and MIR light makes with mixing laser (z-axis). We exploit type-II phase matching (oee) where the upconverted beam and the MIR signal is polarized along the extraordinary axis and the mixing laser is polarized along the ordinary axis of the nonlinear crystal. $n_{e3}(\theta_3,\lambda_3)$ and $n_{e2}(\theta_2,\lambda_2)$ are the angle dependent extraordinary refractive indices of the upconverted and MIR signal, respectively, whereas $n_{o1}(\lambda_1)$ is ordinary refractive index for mixing laser. The angle dependent extraordinary refractive index can be determined as follows;

$$\frac{1}{n_e^2(\theta_i,\lambda_i)} = \frac{\sin^2(\theta_i)}{n_e^2(\lambda_i)} + \frac{\cos^2(\theta_i)}{n_e^2(\lambda_i)} \tag{3}$$

Keeping Δk_L and Δk_T equal to zero, phase matched wavelengths can be calculated as a function of input MIR angles. By rotating the crystal relative to the z-axis, the phase matched wavelength range can be shifted, see Fig.1. *P. Tidemand-Lichtenberg et.al* [13] explained the theory of non-collinear birefringent phase matching in AGS crystal.

Figure 1 shows the phase matched wavelengths as a function of input angles along the x and y axis. Angles in the xz-plane relative to mixing field are denoted by u_i and the corresponding angles along yz-plane are denoted as v_i.

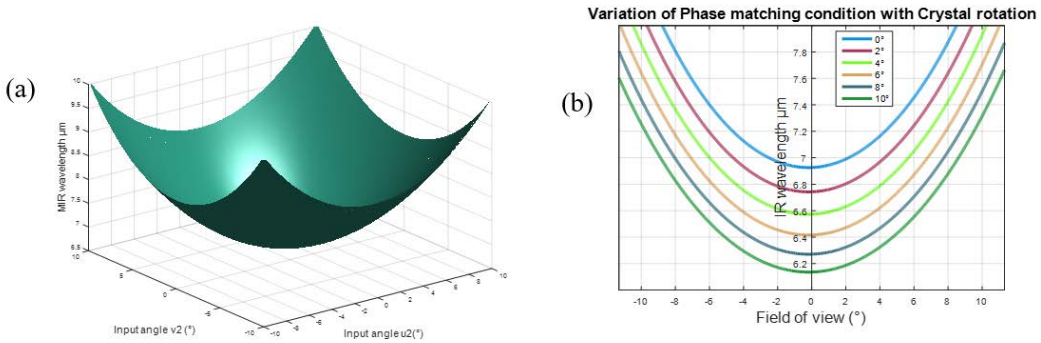

Figure 1: (a) Input angles parallel and normal to the plane formed by $\boldsymbol{k_i}$ and crystal axis vs. phase matched MIR wavelengths (b) Input angles vs. non-collinear phase matched MIR wavelengths at different crystal rotation angles with respect to front facet

Figure 1(b) shows the phase matched wavelengths as a function of u_i while keeping $v_i = 0$ for various crystal rotation angles. It can be understood that by rotating the crystal in the plane of extraordinary axis different ranges of wavelengths can be phase matched allowing for hyperspectral imaging where the full spectrum is measured for every pixel element of the image.

Figure 2 shows the upconversion unit containing the AGS crystal which is a negative uniaxial crystal (5x5x10mm) and the 1064nm diode pumped solid-state laser used as the mixing source. An 808nm diode laser is used to pump the $Nd{:}YVO_4$ crystal generating the 1064nm mixing field, the mirrors M1 and M2 forms the laser cavity. The maximum power output of the mixing laser is approximately 2W. M3 (plane) and M4 (R=200mm) are used to align the mixing laser relative to the nonlinear crystal. The beam diameter into the nonlinear crystal was measured to be ~900µm. The diameter of the mixing laser inside the nonlinear crystal acts as the soft aperture in the Fourier plane of the imaging system setting a limit to the minimum resolvable spatial element of the imaging system. The mixing laser is vertically polarized i.e. polarized along the ordinary axis of the nonlinear crystal.

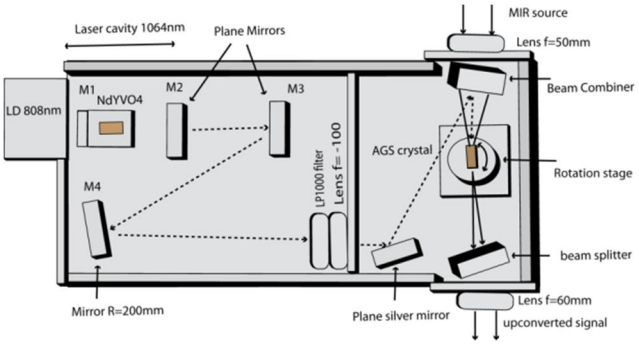

Figure 2: Upconversion unit containing AGS crystal for sum frequency generation. M1 is a concave mirror with curvature R=200mm with high reflection at 1064nm and high transmission at 808nm. M2 is a plane mirror with 90% reflection at 1064nm, and 10% out-coupling. M3 is a plane mirror and M4 is a concave mirror with curvature R=200mm to guide light to the nonlinear crystal. Lens with f=-100mm is used to collimate the converging light.

The AGS crystal used in the setup is optimized for type-II phase matching with a cut angle of $\theta_c = 48°$ with respect to the crystallographic c-axis. The nonlinear crystal has been mounted on a rotation stage so that phase matching condition can be varied by rotating the crystal.

A thermal light source i.e. a globar is used as a broadband MIR illumination source. A beam combiner based on a CaF_2 substrate is used. The beam combiner is designed for high reflection at1064 nm and high transmission for MIR radiations (up to 9µm). A mirror is used as a beam splitter after the upconversion unit to remove the residual 1064nm beam while transmitting the upconverted signal.

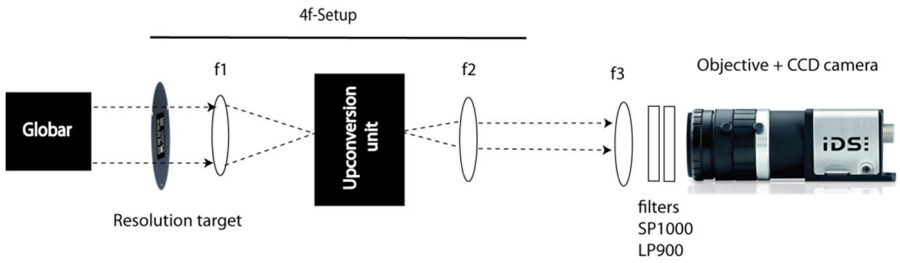

Figure 3: 4f Imaging setup along with the upconversion unit and Si based CCD camera, $\boldsymbol{f_1}$ is to focus the incoming light into the nonlinear crystal, $\boldsymbol{f_2}$ is to collimate the output signal, $\boldsymbol{f_3}$ and objective are to reduce the beam diameter.

Figure 3 demonstrates the 4f imaging system used for spectral imaging. Lens f_1 is a $ZnSe_2$ lens ($f_1 = 50mm$) which is used to transform "position" in the object plane into angle in the Fourier plane, i.e. the back focal plane. The lens f_2 ($= 60mm$) is used to collimate the diverging upconverted light, thereby, back-transforming the angles into positions in the imaging plane. f_3 ($= 35mm$) and the camera objective ($f_4 = 12mm$) are used as beam scaling to optimize the intensity at the camera allowing for shorter integration times of camera. A Polystyrene (PS) film is used as an object carrying spectral features while a United States Air Force (USAF) resolution target is used as an object carrying spatial features. The PS or resolution target is illuminated by thermal radiations emitted from the globar and focused into the nonlinear crystal. It can be seen that the upconversion takes place in the Fourier plane where spatial positions are represented as angles, leading to the radial dependence of the phase matched wavelengths. Due to the relation between radial position and wavelengths, a ring-like image is expected for narrow band illumination and a disk-like image in case of broad band illumination.

RESULTS AND DISCUSSION

Simulated images are created by calculating the intensity distribution at the phase matched wavelengths [15];

$$\boldsymbol{I_{out} \sim \mathrm{sinc}^2\left(\Delta k_L L / 2\pi\right)} \tag{4}$$

Where L=10mm is the length of the nonlinear crystal. The length of the nonlinear crystal limits the angular acceptance bandwidth of the non-collinear phase matching (Eq. 5) [16]

$$\boldsymbol{\Delta\theta = \frac{0.886}{L\tan\theta}\left|\frac{n_{e2}(\theta_2)\left[1-\left(\frac{n_{o2}}{n_{e2}}\right)^2\right]}{\lambda_2\left[1+\left(\frac{n_{o2}}{n_{e2}}\right)^2\tan^2\theta_2\right]}-\frac{n_{e3}(\theta_3)\left[1-\left(\frac{n_{o3}}{n_{e3}}\right)^2\right]}{\lambda_3\left[1+\left(\frac{n_{o3}}{n_{e3}}\right)^2\tan^2\theta_3\right]}\right|^{-1}} \tag{5}$$

The angular acceptance bandwidth for the non-collinear phase matching can be calculated using Equation 5 where L is the crystal length, $n_{ei}(\theta_i)$ is the angle dependent extraordinary refractive index for MIR and upconverted signal, n_{oi} and n_{ei} are the wavelength dependent principle ordinary and extraordinary refractive indices respectively.

A PS film is used since it has absorption lines in 6 to 7 µm wavelength regime. Figure 4(a-b) represent the simulated upconverted images including the spectral features of PS film. The dark regions in the images correspond to PS absorption lines. The images are simulated with the PS film illuminated by collimated, incoherent broadband light.

Figure 5 (a-c) represent the upconverted experimental images achieved from the setup showed in Figure 2 and 3. Figure 5(a) is an upconverted image without PS using a crystal rotation angle ρ=0° i.e. normal incidence of the mixing laser on crystal. Figure 5(b) is obtained with PS spectral features included at ρ=0°, the dark circle in the middle corresponds to absorption line of the PS at 6.9µm (fig.5b). 5(c) shows the upconverted image including the PS spectrum and a crystal angle of ~9.5° (absorption line corresponds to ~6.25µm (Fig.4c)).

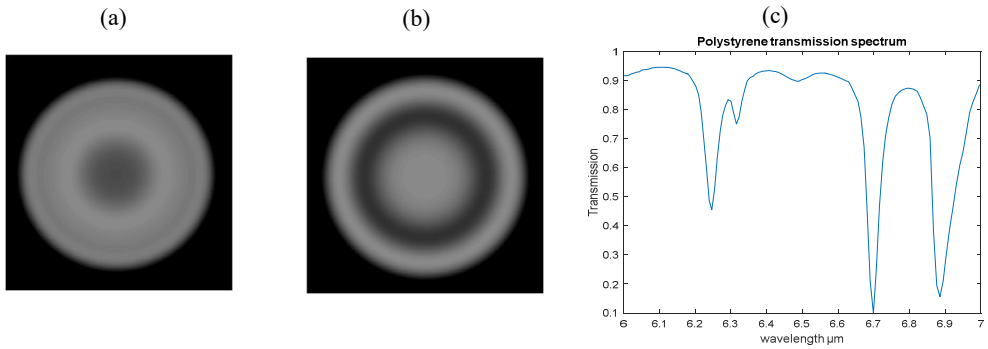

Figure 4: (a) Simulated images with polystyrene spectral features, crystal rotation angle ρ =0° (b) ρ = 9.5°(c) polystyrene transmission spectra (measured with FTIR).

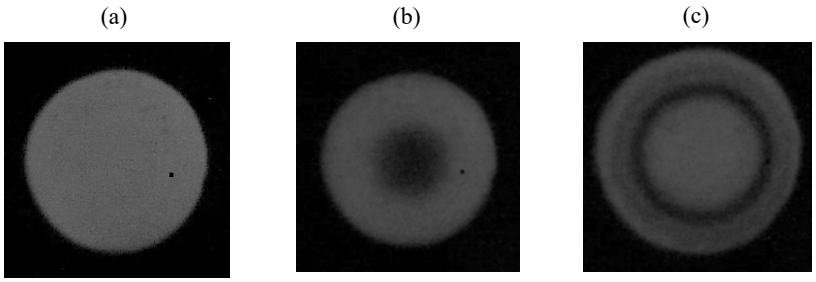

Figure 5: Experimental upconverted images (a) ρ=0° (b) polystyrene spectral features at ρ=0° absorption line corresponds to 6.9µm, (c) polystyrene spectral features at ρ=9.5°, the absorption line corresponds to 6.2µm

As can be seen, the simulated and experimental images are in good agreement (fig. 4(a-b) and 5(b-c)). Since upconversion takes place in the Fourier plane where spatial positions are converted into angles and each angle (between MIR and mixing laser) corresponds to a specific phase matched wavelength. Therefore, variations in spectral brightness of the object (illumination source and PS) results in a radial intensity distribution in the acquired images. When rotating the crystal, the rings converge or diverge within the field of view. The upconverted signal is transformed back to spatial positions via another Fourier transform lens f2 (fig.3).

Since a broadband illumination source is used, the disk-like image is due to several rings each corresponding to specific phase matched wavelengths superimposed with each other. Each phase matched wavelength has an intensity distribution profile resembling a sinc function (radially) with a specific width depending on the longitudinal phase mismatch Δk_L and crystal length L (Eq.4)

A USAF resolution target is used to image the spatial features (clear optical path, Edmund optics).

Figure 6(a) represents the upconverted image of the resolution target illuminated by the globar while figure 6(b) shows the intensity profile in cross section shown in figure 6(a). The magnification between object and image plane can be calculated as;

$$\boldsymbol{IMG}_{(x,y)} = \frac{\boldsymbol{f_2}}{\boldsymbol{f_1}} \frac{\boldsymbol{f_4}}{\boldsymbol{f_3}} \frac{\boldsymbol{\lambda_3}}{\boldsymbol{\lambda_2}} \boldsymbol{OBJ}_{(x,y)} \tag{6}$$

In Eq. 6, f_1, f_2, f_3 and f_4 are focal lengths of the lenses used in the setup (Fig. 3) whereas, the wavelength ratio is directly related to Eq. 2 i.e. transverse phase mismatch. The theoretical scaling factor is calculated to be ~0.062 for 6µm wavelength while the experimental scaling factor can be calculated with the ratio $\frac{43}{561.2} = 0.076$ where 43µm is the distance between 2 lines of the resolution target in the image plane (Fig. 6(b)) and 561.2 µm is that of the object plane.

Using scaling optics on the object side smaller features can be resolved. Also by expanding the beam diameter of the mixing laser inside the nonlinear crystal will improve the resolution of the resolution target. The mixing laser beam diameter inside the nonlinear crystal serves as the soft aperture in the Fourier space which has direct relation with the cut-off spatial frequency to be imaged.

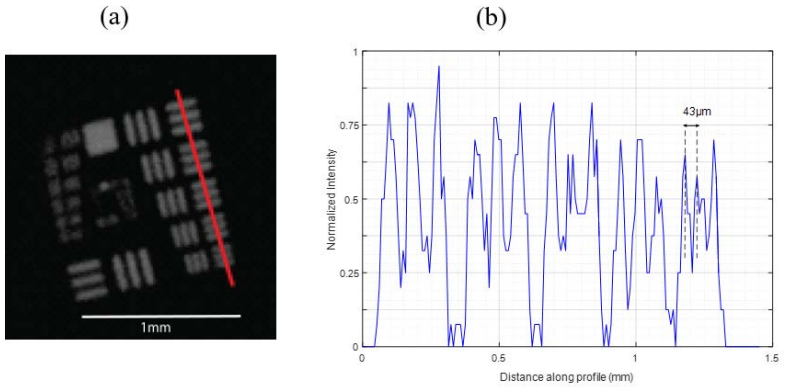

Figure 6: (a) Upconverted image of the resolution target (b) intensity profile across the line drawn on resolution target

CONCLUSION

Nonlinear frequency upconversion has been used to convert the MIR (6-8μm) spectral regime into the visible spectrum where standard CCD cameras are available. The setup used a thermal light source as a broadband illumination source. Passing thermal radiation through the object (PS or resolution target) and then focusing the transmitted light into the nonlinear crystal provides the angles for non-collinear phase matching where every angle corresponds to a specific wavelength. The images achieved will then contain both spatial and spectral information. Scanning the phase matching condition by rotating the crystal has been applied which makes it possible to image every pixel within the field of view including spectral information. After post processing of the acquired images a series of monochromatic images can be reconstructed. Narrow band high intensity illumination sources can also be used where smaller integration times of the camera is needed.

FUNDING : Mid-TECH H2020-MSCA-ITN-2014 grant agreement no:64266

References

[1] A. Lux, "HHT diagnosis by mid-infrared spectroscopy and artificial neural network analysis," *Orphanet J. Rare Dis. 8,* p. 94, 2013.

[2] J. Nallala, "Enhanced spectral histology in the colon using high-maginification benchtop FTIR imaging," *VIBSPE 2610,* 2016.

[3] D. Fernandez, "Infrared spectroscopic imaging for histopathologic recognition," *Nature Biotechnology 23,* pp. 469-474, 2005.

[4] H. Amrania, "Digistain: a digital staining insrument for histopathology," *Optics Express 20,* pp. 7290-7299, 2012.

[5] N. Yamazoe, "Environmental gas sensing," *Sensors and Actuators B, 20,* pp. 95-102, 1994.

[6] G. Song, " Quantitative breath analysis of volatile organic compounds of," *Lung Cancer 67,* pp. 227-231, 2010.

[7] A. Rogalski, "Infrared Detectors," CRC Press, 2010.

[8] J. Midwinter, "Image conversion from 1.6 m to the visible in lithium niobate," *Applied Physics Letters 13,* pp. 68-70, 1968.

[9] J. S. Dam, "Room-temperature mid-infrared single-photon spectral imaging," *Nature Photonics,* pp. 788-793, 2012.

[10] L. M. Kehlet, "Infrared upconversion hyperspectral imaging," *Optics Letters Vol. 40, No. 6,* pp. 938-941, 2015.

[11] L. Hout, "Upconversion imaging using an all-fiber supercontinuum source," *Optics Letters Vol. 41, No. 11,* pp. 2466-2469, 2016.

[12] M. Mathez, "Upconversion imagingusing infrared picosecond pulsed laser source," *Optics Letters,* p. (submitted), 2016.

[13] P. Tidemand-Lichtenberg, "Midinfrared upconversion spectroscopy," *OSA,* vol. B33, pp. D23-D35, 2016.

[14] J. Warner, "Spatial resolution measurement in up-conversion from 10.6μm to the visible," *Applied Physics letters 13,* pp. 360-362, 1968.

[15] J. S. Dam, "Theory for upconversion of incoherent images," *OSA,* 2012.

[16] V.G.Dmitriev, Handbook of Nonlinear Optical Crystals, Springer, 1999.